[13] C. A. Brackett, "The elimination of tuning-induced burnout and bias-circuit oscillation in IMPATT oscillators," *B.S.T.J.*, vol. 52, p. 271, Mar. 1973.
[14] K. Kobayashi, Y Hirachi, K. Ogasawara, A. Shibatomi, and Y. Toyama, "Characteristics of high-power GaAs IMPATT diodes," *Papers of Technical Group on Electron Devices*, IECE., Japan, ED75-61, pp. 19–27, 1975.
[15] Y. Takayama, "Effect of temperature on device admittance of GaAs and Si IMPATT diodes," *IEEE Trans. Microwave Theory Tech.*, vol. MTT-23, p. 673, Aug. 1975.

A New Look at Noise in Transferred Electron Oscillators

HANS R. GNERLICH, MEMBER, IEEE, AND JOHN ONDRIA

Abstract—**Low-frequency current and voltage fluctuations have been measured, and it has been confirmed that noise in packaged transferred electron devices (TED's) is due to three distinct noise mechanisms: flicker, generation–recombination, and thermal noise. For transferred electron oscillators (TEO's), this low-frequency noise is upconverted into the microwave frequency range and adds to the intrinsic RF noise. We have found that between 1 kHz and 1 MHz off the carrier, temperature-dependent generation–recombination noise is the main contributor to the total noise. A model of a noisy TEO is presented. This model permits the calculation of AM and FM noise spectra from device and circuit parameters for measured low-frequency noise or the derivation of device characteristics from noise and circuit parameter measurements.**

I. Introduction

ACKET [1], Copeland [2], DeCacqueray *et al.* [3], and many others have shown that generation–recombination noise is a major contributor to the low-frequency noise of bulk n-GaAs. Sweet [4] found that AM and FM noise is due to intrinsic RF noise, thermal in origin, and "excess noise," a low-frequency noise that is upconverted into the microwave range and has a $1/f$ characteristic. What happened to the generation–recombination noise? The purpose of this investigation is to study the AM and FM noise characteristic of TEO's and identify the physical causes of noise from the measured data. To verify the experimental findings, a simplified model of a nonlinear oscillator is discussed, describing the noise behavior of the TEO in steady-state oscillations.

More than 100 TEO's obtained from various manufacturers have been measured. The data presented are representative of all devices tested.

Manuscript received May 9, 1977; revised July 20, 1977. This work was supported by the US Army Research Office, Durham, NC under Grant DA-ARO-D-31-124-71-G41.

H. R. Gnerlich is with the College of Engineering, the University of South Alabama, Mobile, AL.
J. Ondria is with Lehigh University, Bethlehem, PA.

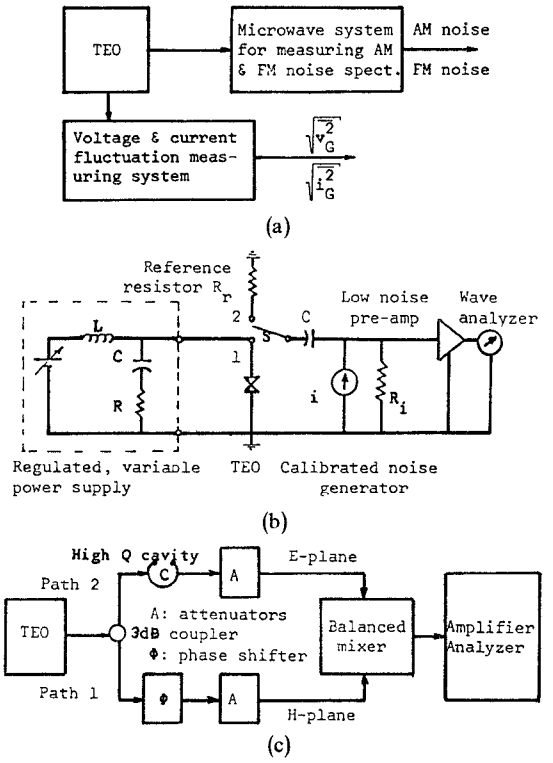

Fig. 1. Noise measuring system. (a) Principle of measurement. (b) Low frequency. (c) Microwave set-up.

II. Measuring System

The experimental work has been performed on n-type GaAs TED's mounted in waveguide cavities. All TED's and cavities are commercially available. At a manufacturer recommended operating voltage, the oscillator is tuned to test frequency 9.28 GHz and matched for optimum power output ranging from 15 to 800 mW.

The noise measuring system (cf. Fig. 1(a)) is used to measure low-frequency TEO noise below and above threshold (cf. Fig. 1(b)). The semiconductor is replaced by an equiv-

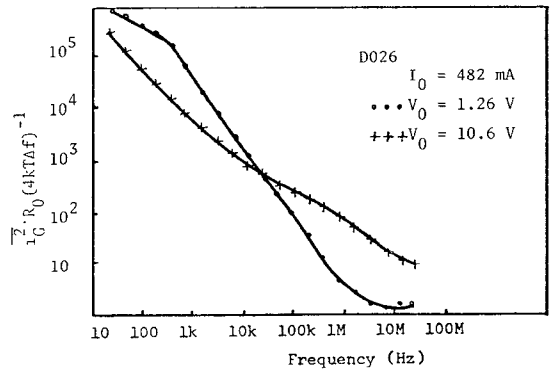

Fig. 2. Normalized low-frequency mean square noise current below and above threshold versus frequency.

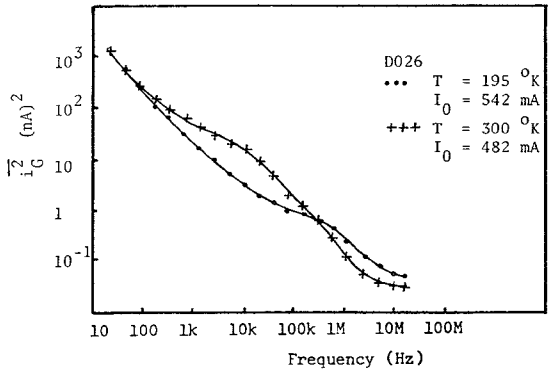

Fig. 3. Mean square noise current versus frequency with temperature as parameter.

alent reference resistor to eliminate the need of knowing quantitatively the measuring system noise figure and gain. The AM–FM noise measuring system, described in detail by Ondria [5] is shown in principle in Fig. 1(c). A noisy signal is demodulated in the balanced mixer. The AM components of the noise sidebands are obtained using path 1 as a direct detection system while path 2 is terminated. The FM components, converted to AM in path 2, are combined in the balanced mixer with the reintroduced, 90 degree phase shifted carrier of path 1.

III. Low-Frequency Noise of TEO's

The low-frequency noise current of TEO's is measured below and above threshold and compared with theoretical spectra of bulk semiconductors.

The mean square noise currents of a TEO, biased above and below threshold, are compared in Fig. 2. The noise caused by trapping centers is dominant. Due to the increase of sample temperature, approximately 100 K above heatsink temperature for the TEO biased above threshold, the contribution of generation–recombination has been shifted from low to high frequencies.

The variation of low-frequency noise with temperature is shown in Fig. 3 for a TEO biased above threshold. The portions of the spectrum due to generation–recombination noise are temperature sensitive, whereas $1/f$ noise is temperature independent. In most cases, we found that the cooling of a TEO increased noise in a frequency range approxi-

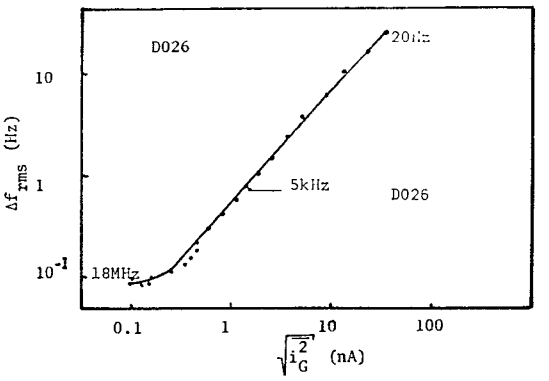

Fig. 4. Correlation of low-frequency noise current and frequency deviation per 1-Hz bandwidth. Frequency is parameter and increases from right to left by octaves.

mately 1 kHz–100 kHz. We were able to identify three separate noise mechanisms in the frequency range from 20 Hz to 18 MHz: 1) flicker noise for frequencies below 10 kHz, 2) generation–recombination noise between 1 kHz and 10 MHz, and 3) thermal noise above 1 MHz.

Using the theoretical mean square noise current in bulk semiconductors and curve fitting techniques, the time constants τ associated with generation–recombination noise were determined. Typically, we obtained values of τ at 300 K to be approximately 15 ms, 4 ms, and between 2 and 4 μs. This agrees with findings by Acket [1] and Copeland [2].

IV. AM and FM Noise in TEO's

Measured AM and FM noise of TEO's mounted in waveguide cavities is compared with the low-frequency noise of these devices.

For a modulating frequency range, 20 Hz $< f_m <$ 18 MHz, the correlation between low-frequency noise current $\sqrt{\overline{i_G^2}}$ and frequency deviation Δf_{rms} is shown in Fig. 4. A smooth curve drawn through the measured points follows approximately a straight line from 20 Hz to 1 MHz, described by

$$\Delta f_{\text{rms}} = M_{FI} f_{10} Q_L^{-1} \sqrt{\overline{i_G^2}}. \tag{1}$$

For known RF frequency f_{10} and loaded quality factor Q_L, the frequency modulation sensitivity due to current fluctuations M_{FI} can be determined from the graph. Where Δf_{rms} is independent of low-frequency current fluctuations, FM noise is only due to intrinsic RF noise. From this value of Δf_{rms}, equivalent noise temperature [6] T_n can be estimated. (For all devices measured we found $8 < M_{FI} < 19$ and 7000 K $< T_n <$ 26 000 K).

Low-frequency noise current $\sqrt{\overline{i_G^2}}$ produces bias voltage fluctuations $\sqrt{\overline{v_G^2}}$ across the low-frequency admittance. Adding parallel conductances across the oscillator bias terminals changes the voltage fluctuations (cf. Fig. 5) and therefore the upconverted noise (cf. Fig. 6). Correlation of low-frequency voltage fluctuations and FM noise are shown in Fig. 7, for $R = 25\,\Omega$ and $R = 1500\,\Omega$. For the greater value of R, upconverted noise dominates, and intrinsic RF noise cannot be detected.

An increase of bias resistance increases the amount of bias

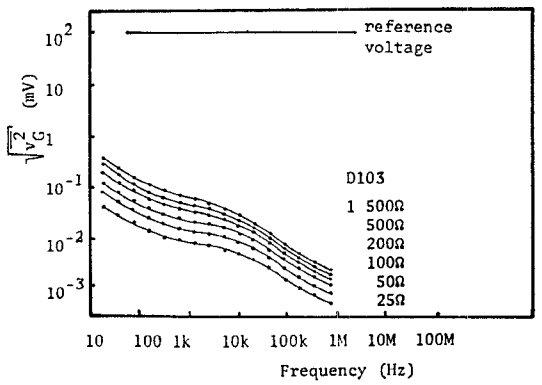

Fig. 5. Noise voltage per 1-Hz bandwidth versus frequency. Bias resistance parameter.

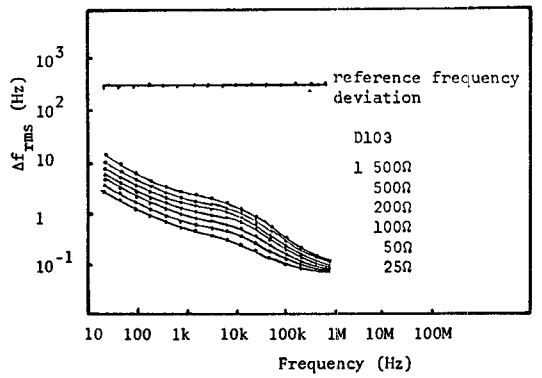

Fig. 6. Frequency deviation per 1-Hz bandwidth versus frequency. Bias resistance is parameter.

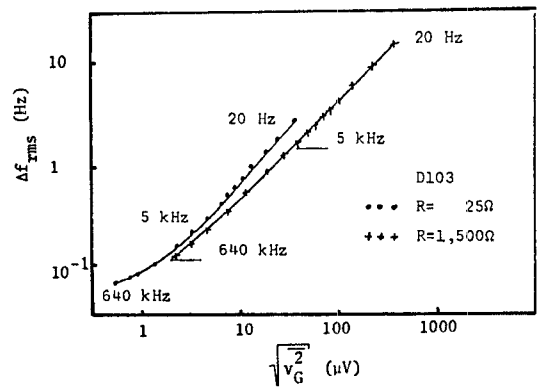

Fig. 7. Correlation of low-frequency noise voltage and frequency deviation, per 1-Hz bandwidth. Frequency is parameter and increases from right to left by octaves.

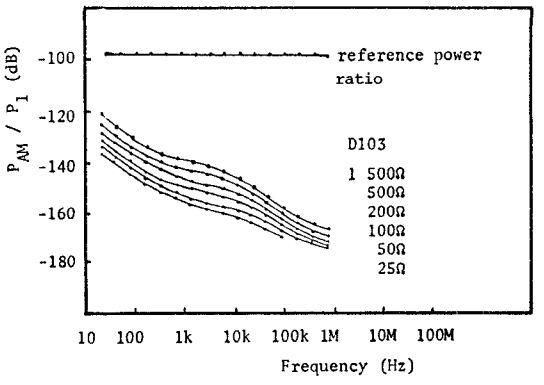

Fig. 8. AM noise spectrum per 1-Hz bandwidth versus frequency. Bias resistance is parameter.

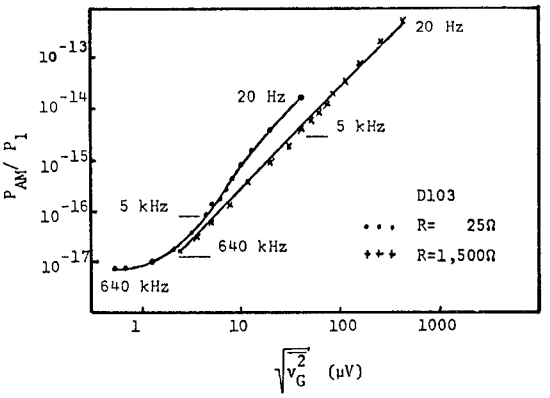

Fig. 9. Correlation of low-frequency noise voltage and AM noise power. Frequency is parameter and increases from right to left by octaves.

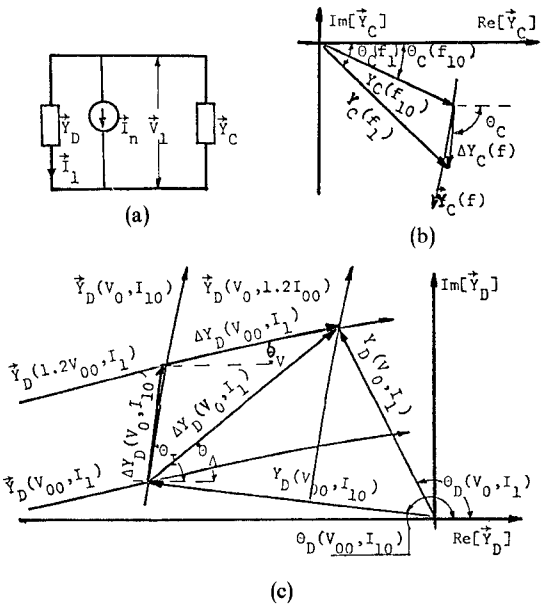

Fig. 10. TEO. (a) Model of TEO at fundamental frequency f_1. (b) Circuit admittance as function of RF frequency. (c) TED admittance as function of RF current and bias voltage.

fluctuations (cf. Fig. 5) and, therefore, AM noise (cf. Fig. 8). Correlation between AM noise and low-frequency noise voltage is shown in Fig. 9. For large input impedance, the amount of upconverted noise is much larger than intrinsic noise. AM and low-frequency noise are proportional. (The change in slope of the $R = 25\ \Omega$ curve is not understood at this time.)

V. An Equivalent Circuit for TEO's

To verify our experimental findings, a simplified model [7], [8] of a nonlinear oscillator is discussed, describing the noise behavior of the TEO in steady-state oscillations. Since the active part of a TED is usually small compared to its wavelength in free space, a current–voltage equivalent circuit for the fundamental frequency of oscillation is defined at the active device terminals. The TED (cf. Fig. 10) is represented by admittance $\vec{Y}_D$, free of intrinsic noise, in parallel

with noise current generator $\vec{I}_n$. The circuit and load admittance $\vec{Y}_C$ is transformed by the diode package to the TED terminals.

The condition for stable oscillations is

$$\vec{I}_n + \vec{V}_1[\vec{Y}_D(V_0,I_1) + \vec{Y}_C(f_1)] = 0 \tag{2}$$

where V_0 is the bias voltage, I_1, V_1, and f_1 are RF current, voltage, and frequency, respectively. Substituting magnitude and phase angle, defined in Fig. 10, (2) can be solved for the RF variations

$$\Delta I_1 = \frac{\frac{\partial \Delta Y_D}{\partial V}\sin(\theta_V - \theta_C)\Delta V_0 + \frac{Y_D}{I_{10}}\sin(\theta_n + \theta_D - \theta_C)I_n}{\frac{\partial \Delta Y_D}{\partial I}\sin(\theta_I - \theta_C)} \tag{3}$$

$$\Delta f_1 = \frac{\frac{\partial \Delta Y_D}{\partial V}\sin(\theta_I - \theta_V)\Delta V_0 + \frac{Y_D}{I_{10}}\sin(\theta_I - \theta_n - \theta_D)I_n}{\frac{d\Delta Y_C}{df}\sin(\theta_I - \theta_C)} \tag{4}$$

which are linear functions of low-frequency variations ΔV_0 and RF noise $I_n(t)$. Referred to double sidebands, noise to carrier power ratio

$$\frac{P_{AM}}{P_1} = B[M_A^2\Delta V_0^2(f_m) + T_A^2 I_n^2(f_m)] \tag{5}$$

and rms frequency derivation

$$\Delta f_{\text{rms}} = \frac{f_{10}}{Q_L}[B(M_F^2\Delta V_0^2(f_m) + T_F^2 I_n^2(f_m))]^{1/2} \tag{6}$$

can be calculated [8] from the spectral densities of ΔI_1 and Δf_1. Amplitude modulation sensitivity

$$M_A = \frac{\partial \Delta Y_D}{\partial V}\sin(\theta_V - \theta_C)\left[I_{10}\frac{\partial \Delta Y_D}{\partial I}\sin(\theta_I - \theta_C)\right]^{-1} \tag{7}$$

the transformation coefficient of RF noise current to AM noise power

$$T_A = Y_D\left[I_{10}^2\frac{\partial \Delta Y_D}{\partial I}\sin(\theta_I - \theta_C)\right]^{-1} \tag{8}$$

loaded oscillator quality factor

$$Q_L = f_{10}\frac{d\Delta Y_C}{df}\sin(\theta_I - \theta_C)\{2\ \text{Re}\ [Y_C(f_{10})]\}^{-1} \tag{9}$$

frequency modulation sensitivity

$$M_F = \frac{\partial \Delta Y_D}{\partial V}\sin(\theta_I - \theta_V)\{\sqrt{2}\ \text{Re}\ [Y_C(f_{10})]\}^{-1} \tag{10}$$

and transformation coefficient of RF noise current to rms deviation

$$T_F = Y_D\{\sqrt{2}I_{10}\ \text{Re}\ [Y_C(f_{10})]\}^{-1}. \tag{11}$$

Since AM and FM noise have the same origin, a cross spectrum

$$\begin{aligned}\overline{\Delta I_1 \Delta f_1} = {} & \left[\frac{\partial \Delta Y_D}{\partial I}\frac{d\Delta Y_C}{df}\sin^2(\theta_I - \theta_C)\right]^{-1} \\ & \cdot \left\{\left[\left(\frac{\partial \Delta Y_D}{\partial V}\right)^2 \sin(\theta_V - \theta_C)\sin(\theta_I - \theta_V)\right]\overline{\Delta V_0^2}\right. \\ & + \frac{Y_D}{I_{10}}\frac{\partial \Delta Y_D}{\partial V}\overline{[\cos(\theta_I + \theta_C - \theta_n - \theta_D - \theta_V)} \\ & \left. - \overline{\cos(\theta_I - \theta_C)\cos(\theta_V - \theta_n - \theta_D)]\Delta V_0 I_n} \right. \\ & \left. + \left(\frac{Y_D}{I_{10}}\right)^2 \overline{\sin(\theta_n + \theta_D - \theta_C)\sin(\theta_I - \theta_n - \theta_D)I_n^2}\right\}\end{aligned} \tag{12}$$

results. The cross-correlation coefficient

$$\gamma = \overline{\Delta I_1 \cdot \Delta f_1}[\overline{\Delta I_1^2 \cdot \Delta f_1^2}]^{-1/2} \tag{13}$$

was evaluated from case to case.

VI. Discussion of Results

Equations (5) and (6) verify our experimental findings. A reference voltage, high compared to noise (cf. Fig. 5), is applied across the TEO bias terminals, and reference frequency deviation and power ratio are measured (dots) (cf. Figs. 6 and 8), respectively; the solid lines in these figures are calculated by multiplying the reference voltage with FM or AM upconversion factors, determined from device and circuit parameters. Measured values and those calculated using equations (5) and (6) are in good agreement.

Low-frequency fluctuations that vary in magnitude, compared to the intrinsic RF-noise current, are obtained by varying a resistance across the TEO supply leads (cf. Fig. 5). Where low-frequency fluctuations are large compared to intrinsic RF noise, FM and AM noise and low-frequency fluctuations are proportional (cf. Figs. 7 and 9); FM and AM noise spectra become independent of low-frequency fluctuations where RF noise is dominant.

VII. Conclusions

1) Generation–recombination noise contributes to the total noise of TEO's between approximately 1 kHz and 1 MHz off the carrier. We have identified the impurities causing the trapping centers of this noise. Control of the impurities during manufacturing will reduce the total noise.

2) Measurements of low-frequency noise, less costly than RF-noise measurements, give an indication of AM and FM noise spectra to be expected.

3) The model of a noisy TEO permits calculation of AM and FM noise spectra from circuit and device parameters for known measured low-frequency noise. Close to the carrier, where AM and FM noise is proportional to low-frequency noise, (5) and (6) become simple to use.

4) Work is in progress to determine circuit and/or device parameters from low-frequency and RF-noise measurements.

ACKNOWLEDGMENT

The authors wish to thank C. B. Winn who helped with the measurements.

REFERENCES

[1] G. A. Acket, "Recombination and trapping in epitaxial N-type gallium arsenide," *Phillips Research Reports*, vol. 26, pp. 261–278, 1971.
[2] J. A. Copeland, "Semiconductor impurity analysis from low frequency noise spectra," *IEEE Trans. Electron Devices*, vol. ED-18, pp. 50–53, Jan. 1971.
[3] A. DeCacqueray, G. Glasquez, and J. Graffeuil, "Etude du Bruit de Generation Recombination de Diodes Gunn," *Solid-State Electronics*, vol. V, no. 16, pp. 853–860, Aug. 1973.
[4] A. A. Sweet and L. A. Mackenzie, "FM noise in CW gunn oscillators," *Proc. IEEE*, May 1970.
[5] J. G. Ondria, "A microwave system for measurement of AM and FM noise spectra," *IEEE Trans. Microwave Theory Tech.*, vol. MTT-16, pp. 767–781, Sept. 1968.
[6] A. Ataman and W. Harth, "Intrinsic FM noise of gunn oscillators," *IEEE Trans. Electron Devices*, vol. ED-20, pp. 12–14, Jan. 1973.
[7] M. S. Gupta, "Noise characteristics of avalanche transit time microwave diodes," Ph.D. dissertation, University of Michigan, 1972.
[8] H. R. Gnerlich, "Noise in transferred electron oscillators," Ph.D. dissertation, Lehigh University, 1975.

Design of GaAs MESFET Oscillator Using Large-Signal *S*-Parameters

YASUO MITSUI, MASAAKI NAKATANI, AND SHIGERU MITSUI

Abstract—**A design method of GaAs MESFET oscillator using large-signal *S*-parameters has been discussed. Together with the measurement results of the dependence of large-signal *S*-parameters on power levels and bias conditions, computer analysis of the equivalent circuit for MESFET's has qualitatively clarified the large signal properties of MESFET's. On the basis of these findings, *S*-parameters have been designed for the MESFET oscillator over the frequency range of 6–10 GHz, which has resulted in power output of 45 mW at 10 GHz with 19-percent efficiency, and 350 mW at 6.5 GHz with 26-percent efficiency, respectively.**

Good agreements between predicted and obtained performances of MIC positive feedback oscillator have been ascertained, verifying the validity of the design method using large-signal *S*-parameters.

I. INTRODUCTION

EXCELLENT performances of GaAs Schottky gate-field effect transistors (GaAs MESFET's) in frequency [1], [2] and power [3]–[5] have provoked microwave systems engineers to design GaAs MESFET oscillators [6]–[8] as a local oscillator or a microwave power source. Since microwave oscillators using GaAs MESFET's operate under a large-signal condition, circuit designers have been forced to utilize cut and try methods to achieve the optimum design, modifying the design with small-signal *S*-parameters.

This paper describes a successful design method of low-noise GaAs MESFET oscillators using measured large-signal *S*-parameters [9]. In Section II, the measurement and applicability of large-signal *S*-parameters of *X*-band GaAs MESFET are represented, and, together with the equivalent circuit analysis, large-signal properties of FET's are discussed qualitatively. Then some of the limitations of large-signal *S*-parameters on the design of the oscillator are deduced. The detailed design considerations of oscillators are presented in Section III. In Section IV, some experimental results of designed oscillators are shown, and good agreements between predicted and obtained performances are ascertained, verifying the validity of the design method using large-signal *S*-parameters.

Manuscript received May 16, 1977; revised July 3, 1977.
The authors are with the Mitsubishi Electric Corporation, Itami, Hyogo, Japan.

II. LARGE-SIGNAL *S*-PARAMETERS

Each transistor used in this experiment has a 1-μm long and 300-μm wide gate, a channel doping of 7–9 $\times 10^{16}$ cm^{-3} and pinch-off voltage of 4.0 V nominally, which is mounted in a microdisk package.

Large-signal *S*-parameters, if measured, could be used to calculate gate and drain RF current amplitudes $|\tilde{i}_{gs}|$ and $|\tilde{i}_{ds}|$ as a function of the available power of signal generator P_I:

$$P_I = |a_i|^2, \qquad i = 1, 2 \tag{1}$$

$$S_{11} = \left(\frac{b_1}{a_1}\right)_{a_2=0} = \frac{Z_{L1} - Z_0}{Z_{L1} + Z_0} \tag{2}$$

$$P_I(1 - |S_{11}|^2) = \tfrac{1}{2} \operatorname{Re}(Z_{L1})|\tilde{i}_{gs}|^2 \tag{3}$$

$$S_{22} = \left(\frac{b_2}{a_2}\right)_{a_1=0} = \frac{Z_{L2} - Z_0}{Z_{L2} + Z_0} \tag{4}$$

$$P_I(1 - |S_{22}|^2) = \tfrac{1}{2} \operatorname{Re}(Z_{L2})|\tilde{i}_{ds}|^2 \tag{5}$$

where Z_{L1},Z_{L2} are the input and the output impedances of FET and $Z_0 = 50\ \Omega$.